

UV-Cured Membranes for Gas Separation

Luke Kwisnek, * Charles E. Hoyle, Sergei Nazarenko

School of Polymers and High Performance Materials
The University of Southern Mississippi, Hattiesburg, MS 39406

Abstract: UV-curable thiol-based chemistries were used to fabricate polymeric membranes for separating carbon dioxide from gaseous mixtures. Correlations were made based on network functionality, architecture, and the resulting gas transport properties. CO₂, oxygen, nitrogen, and methane permeability were studied as a function of testing temperature and input pressure for each membrane. Such membranes can be used for gas purification or atmospheric scrubbing for life support systems and environmental sustainability.

Introduction

Gas separation (GS) membranes are an eco-friendly, cost effective method to separate gaseous mixtures.¹ Such membranes can be produced and operated inexpensively in order to replace costly, and in some cases polluting, commercial gas separation techniques such as distillations or amine treatments. Natural gas purification, hydrogen recovery, air separation, atmospheric scrubbing, and dehydration are some of the more common applications for GS membranes.¹ In 1991,² and later updated in 2008,³ Robeson reported an upper-bound limit between the permeability of polymer membranes and their permselectivity for different gases. He demonstrated that a trade-off exists between the two properties. For high selectivity one must sacrifice flux (productivity) and vice versa.^{2,3} Naturally there is an industrial interest in developing membranes that beat the upper bound limit, i.e. a membrane with high permeability *and* high selectivity.

GS membranes operate on the principle of selective permeation or permselectivity. According to the solution-diffusion equation ($P = D \cdot S$), there are two components which may be tuned to increase permselectivity: diffusivity selectivity (D_A/D_B) and solubility selectivity (S_A/S_B) (1):⁴

$$\frac{P_A}{P_B} = \left(\frac{D_A}{D_B} \right) \left(\frac{S_A}{S_B} \right) \quad (1)$$

Zeolite molecular sieves are known for their uniform and fixed pore sizes which separate small molecules based on diffusivity, or size, selectivity. Because zeolite membranes are expensive and relatively fragile, high- T_g , glassy polymers with rigid backbones such as polyimides have been explored for diffusivity selective membranes.⁴

Solubility selectivity, or affinity selectivity, is another route by which gas mixtures containing polar gases like CO₂ and H₂S can be separated. The great advantage of solubility selective membranes is that rubbery, low T_g polymers with extremely high permeabilities can be used since the permselectivity is based on chemical affinity rather than size. In particular, poly(ethylene glycol) (PEG)-based polymer membranes have a very high solubility-selectivity for CO₂ transport.⁶ The polar ethylene glycol repeat units have a strong affinity for CO₂ molecules which have quadrupolar moments.⁶

This affinity increases the permeability of CO₂ through the membrane dramatically compared with other gases like N₂, O₂, CH₄ and even H₂, which is a reverse-selective process due to H₂ being smaller in size than CO₂.⁶

GS membranes are processed typically by solution-casting and hollow-fiber spinning.⁴ In rare instances, UV-curing has been used to fabricate membranes.^{6,7} UV-photopolymerization is a rapid, efficient, and well-established method of curing liquid monomers and oligomers into solid polymer films.^{8,9} The advantages of UV-curing are widely known: rapid processing of large areas of material, tunable properties since a wide variety of acrylated oligomers and thiol-enes are available, eco-friendly due to 100% reactive components (no solvents) and high energy efficiency, and the flexibility of coating to a variety of substrates or as free-standing films.^{8,9} UV-curable membranes might also be used to repair defects in existing GS membranes or as coatings which enhance their performance.

In this work, the permeabilities of oxygen, nitrogen, and carbon dioxide in UV cured thiol-based films were evaluated. Diffusivity, *D*, and solubility, *S*, were decoupled from the permeability, *P*, in order to verify the source of permselectivity. Advantages of multifunctional thiols in an acrylate mixture are demonstrated.

Experimental

Materials

The thiol monomers glycol di(3-mercaptopropionate) (2T) pentaerythritol tetra(3-mercaptopropionate) (4T) were supplied by Bruno Bock Thio-Chemical-S. Acrylate oligomer poly(ethylene glycol) diacrylate (PEGDA) with average $M_n = 700$ g/mol was obtained from Aldrich. All mixtures were initiated using the photoinitiator 1-hydroxycyclohexyl-phenyl ketone (HCPK, or Irgacure 184) supplied by Ciba Specialty Chemicals. All materials were used as received.

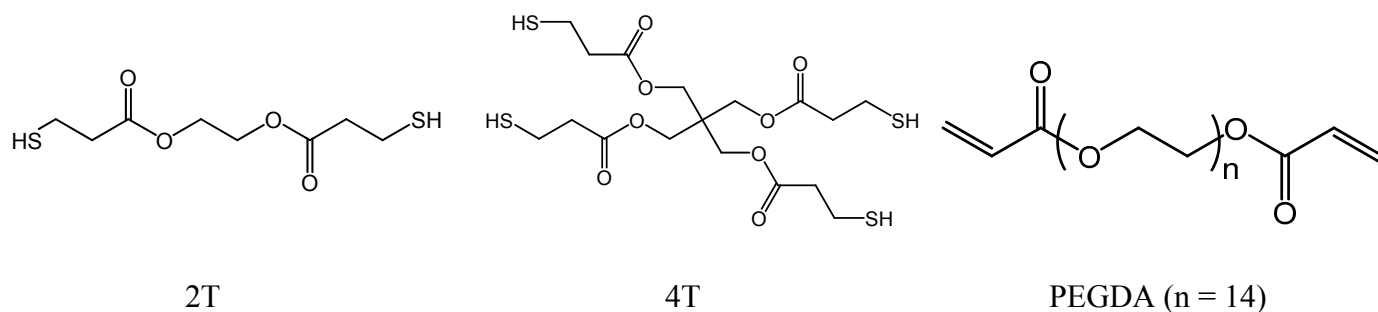


Figure 1. Structures of thiol monomers and acrylate oligomer.

Preparation of films

For the control material, PEGDA, 1 wt% HCPK was added to the PEGDA and then sonicated for 10 minutes. This mixture was then poured onto a glass plate and sandwiched by another glass plates with a 1mm shim to control the thickness. This glass plate/oligomer sandwich was then cured using 10 passes at 10 ft/min feed speed under a Fusion UV curing line system with a D bulb (400W/cm² with belt speed of 10 feet/min and 3.1 W/cm² irradiance). For thiol-acrylate mixtures, 20 mol% (based on total

functional groups, i.e. $-\text{SH} = 1$, acrylate = 1) of thiol was added to PEGDA. HCPK was then incorporated at 1 wt%, sonicated, and cured as already described. This procedure was used both with 2T as the thiol additive and 4T as the thiol additive.

Characterization

Permeation of oxygen and carbon dioxide were measured using a custom-built gas permeation analyzer based on a constant-volume, variable pressure (manometric) technique. Upstream feed gas pressure was measured and monitored with an Omega Engineering pressure transducer. Downstream permeated gas pressure was monitored with an MKS 226A differential pressure transducer. Both transducers were connected to a computer for real-time data collection. Permeation cells were maintained at a constant 23 °C via a recirculating chiller. All film samples were degassed using high vacuum for 24 hours prior to testing.

Functional group conversions for all networks were monitored using a Bruker 88 FTIR spectrometer modified with a fiber-optic cable to irradiate samples sandwiched between two salt plates. The conversion of acrylate double bonds at 810 cm^{-1} were monitored as a function of irradiation time. An Oriel 200 W high-pressure mercury-xenon lamp with light intensity of 6.16 mW/cm^2 at 365 nm was used to irradiate the samples and invoke photopolymerization. Both air and nitrogen curing atmospheres were investigated.

Tack-free time studies for films cured in sunlight were conducted on the roof of the USM School of Polymers and High Performance Materials building. Films were drawn down at 4 mil thickness onto steel substrates. Solar radiation was 90 mW/cm^2 and the UV index was 10 as recorded by a Davis Advantage Pro 2 weather station.

Results and Discussion

A typical experimental permeation curve using the technique described in the Experimental section is shown in Figure 2. This example specifically is a 640 micron PEGDA control membrane tested for CO_2 permeability. The black line is experimental data reported by the differential pressure transducer. The red line is the fit to the steady-state slope and is used to calculate P .

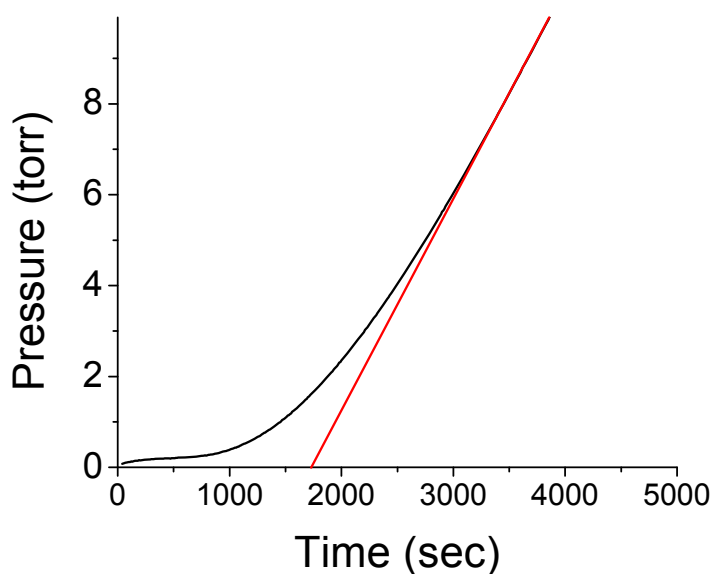


Figure 2. Actual fickian flux curve for CO₂ permeation through a 640 micron PEGDA membrane. Black line is experimental data for permeated gas pressure while red line is the fit to the steady-state slope allowing the calculation of the permeability, P .

From these curves, permeability values for O₂ and CO₂ for each membrane were generated and are listed in Table 1.

| | P _{O₂} (Barrer) | P _{CO₂} (Barrer) | Selectivity (P _{CO₂} /P _{O₂}) |
|-----------------|--|---|---|
| PEGDA | 2.6 | 40 | 16 |
| PEGDA+2T | 2.1 | 40 | 19 |
| PEGDA+4T | 1.8 | 30 | 17 |

Table 1. Permeabilities for O₂ and CO₂ and the selectivity measured at 23 °C.

No difference in the permeability for CO₂ was observed for the PEGDA+2T modified network, while a slight decrease in CO₂ permeability was measured for the PEGDA+4T modified network which could be due to restrictions in mobility because the 4T is a tetrafunctional crosslinker which likely increases the crosslink density of the membrane. However, the selectivities for each material are quite comparable and in fact slightly improved for the PEGDA+2T modified network.

Acrylate group conversions were studied as a function of UV irradiation time as described in the experimental section. As expected, under a nitrogen atmosphere all three networks rapidly reached 100% conversion of acrylate groups as shown in Figure 3. Actual spectra from the first (pre-curing) IR scan, a mid-conversion scan, and a fully-cured scan are provided as insets.

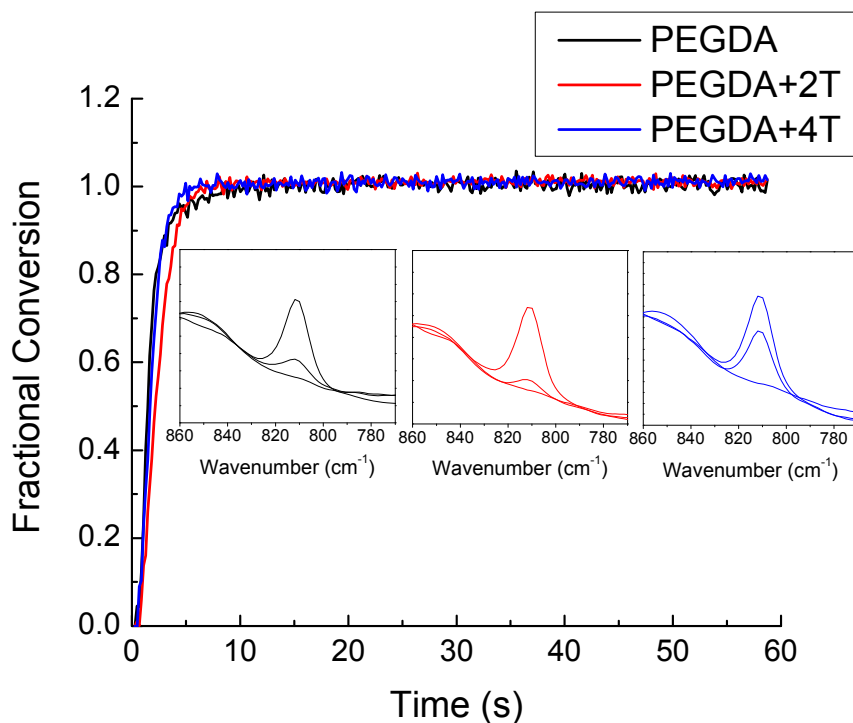


Figure 3. Fractional conversion of acrylate functional groups for three networks under nitrogen atmosphere.

Note that in these networks, the acrylate double bonds homopolymerize while the thiols add into the acrylate double bonds; these reactions happen simultaneously. No measurable differences in rate or total conversion were expected or observed. However without a nitrogen blanket, i.e. in ambient air, the fractional conversions of each network show striking differences as seen in Figure 4.

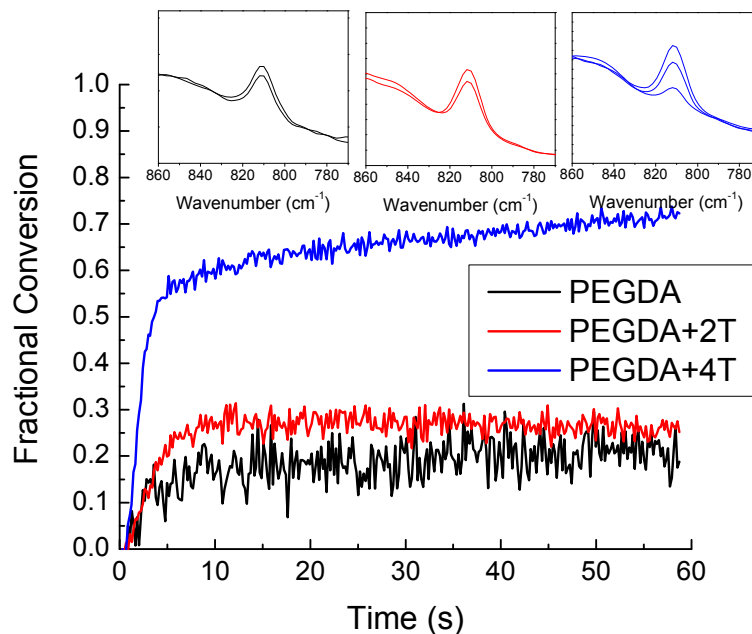


Figure 4. Fractional conversion of acrylate functional groups for three networks under ambient air atmosphere.

Both the PEGDA control network and the PEGDA+2T thiol-modified network reach low acrylate conversions even after 60 seconds. In contrast, the PEGDA+4T thiol-modified network attains 50% conversion after only 5 seconds and nearly 70% conversion after 60 seconds. This result demonstrates the utility of incorporating a multifunctional thiol crosslinker into a PEG-based diacrylate oligomer when curing in an air (oxygen) atmosphere. The free-radical, step-growth thiol-ene reaction has very low oxygen inhibition while the free-radical, chain-growth acrylate homopolymerization reaction is hindered by oxygen due to the formation of unreactive peroxy radicals.¹⁰

To further demonstrate the energy efficiency and eco-friendly advantages of the thiol-ene reaction, tack free time studies were performed on 4 mil thick films of each network using sunlight in outdoor ambient air. As seen in Table 2, sunlight is able to cure the thiol-modified networks as compared to the PEGDA control which was still tacky on the surface after nearly 4 hours. This is in contrast to the PEGDA+4T membrane which left no tack after only 5.5 minutes.

| Material | Tack-free Time (sec) |
|----------|----------------------|
| PEGDA+4T | 330 |
| PEGDA+2T | 900 |
| PEGDA | 14000+ |

Table 2. Tack free times for each membrane when cured with sunlight under ambient outdoor air conditions.

The tack-free time studies, along with the curing atmosphere investigations using RT-FTIR, demonstrate that acrylate-based UV-curable membranes may be fabricated in air and at faster line speeds (less UV light intensity) during commercial production.

Conclusions

UV-photopolymerized thiol-acrylate membranes were fabricated and tested for CO₂/O₂ separation performance. While indicating no significant improvement in this regard, the incorporation of multifunctional thiols to PEG-based acrylated oligomers allowed for air atmosphere curing and also sunlight curing outdoors instead of a UV lamp source, demonstrating the environmental friendliness and energy efficiency of this approach. Present work is aimed at developing and testing new thiol-based, UV-curable network designs for CO₂ gas separation. Correlations between crosslinking density, ethylene glycol content, feed gas pressure, and membrane performance and durability will be demonstrated in the presentation.

References

1. Bernardo, P.; Drioli, E.; Golemme, G. *Ind. Eng. Chem. Res.* **2009**, *48*, 4638.
2. Robeson, L. M.; *J. Membr. Sci.* **1991**, *62*, 165.
3. Robeson, L. M.; *J. Membr. Sci.* **2008**, *320*, 390.
4. Koros, W. J.; Coleman, M. R.; Walker, D. R. B. *Annu. Rev. Mater. Sci.* **1992**, *22*, 47.
5. Breck, D. W. *Zeolite Molecular Sieves: Structure, Chemistry, and Use*. John Wiley & Sons, New York, 1974.
6. Lin, H.; Freeman, B. D. *J. Mol. Struct.* **2005**, *739*, 57.
7. Tiemblo, P.; Guzman, J.; Riande, E.; et al. *Journal of Polymer Science Part B: Polymer Physics*, *39*, 786-795, 2001.
8. Hoyle, C. E., Kinstle, J. F. *Radiation Curing of Polymeric Materials*, American Chemical Society, Washington D.C., **1990**.
9. Jacobine, A. F. In *Radiation Curing in Polymer Science and Technology*; Fouassier, J. P., Rabek, J. F., Eds.; Elsevier Applied Science: London, **1993**; Vol. III, pp 219–268.
10. Hoyle, C. E.; Lee, T.Y.; Roper, T. *J. Polym. Sci., Part A: Polym. Chem.* **2004**, *42*, 5301.